Journal of the Optical Society of Korea, Vol. 10, No. 4, December 2006, pp. 178-183

Three Dimensional Shape Measurement of a Micro Fresnel Lens with In-line Phase-shifting Digital Holographic Microscopy

Jeon Woong Kang and Chung Ki Hong*

Department of Physics, Pohang University of Science and Technology, Pohang 790-784, Korea

(Received November 2, 2006 : revised November 2, 2006)

An in-line phase-shifting digital holographic microscopy system was constructed by inserting a conventional microscope in the object arm of a Mach-Zehnder interferometer. It was used to measure the three dimensional shape of a micro Fresnel lens. It was also shown that both the lateral and the axial resolutions of the in-line phase-shifting system using a self-calibration algorithm were superior to those of the best off-axis system.

OCIS codes : 090.2880, 100.2000

I. INTRODUCTION

Three-dimensional shape measurement of microscopic objects is important in many fields such as biology, micro-electronics industry, and MEMS engineering. Scanning confocal microscopy has been used for this purpose, but the process of the three-dimensional scanning is rather time-consuming [1]. Microscopic electronic speckle pattern interferometry can provide the three-dimensional information with a whole-field measurement, but it requires a focusing mechanism to record speckle patterns at various field depths [2]. This problem has prevented its application to the observation of objects with a considerable thickness or axial movement.

In digital holography, many holograms can be recorded with a CCD in a matter of sub-seconds and the images of the object are reconstructed numerically afterwards. Because the focusing can be adjusted in the reconstruction process, digital holography is free from the process of mechanical focusing and can be used to monitor the dynamic change of objects.

A digital holographic system can be configured in off-axis or in-line setup. The off-axis system has a great advantage over the in-line setup because it requires only a single hologram to generate the object image and, therefore, it can be used to monitor objects in-situ. But, the drawback of the off-axis system is that about a half of the CCD pixels are filled with the carrier fringes and the distance between the object and the CCD must be long enough to separate the reconstructed object image from the useless zero-order. As a result, the numerical aperture of the imaging optics is reduced and the obtained image is of low resolution. These problems can be solved by configuring the holographic system in in-line setup [3-5].

An in-line digital holographic system has another advantage, which is that phase-shifting methods can be employed to measure the complex object field on the CCD plane. The complex object image reconstructed from it can have better phase resolution than that can be obtained with off-axis systems by a factor of two. Therefore, an in-line phase-shifting digital holography system is more useful in the precision shape measurement of transparent objects whose thickness or height profiles are proportional to the phase profiles of their complex images.

In this paper, we present the result of the shape measurement of a micro Fresnel lens done with an in-line phase-shifting digital holographic system. We also show that both transverse and axial resolutions of our system are better than those of previous off-axis systems [6-8].

II. IN-LINE PHASE-SHIFTING DIGITAL HOLOGRAPHIC MICROSCOPY

The schematic of the in-line phase-shifting digital holographic microscopy system is shown in Fig. 1. A linearly polarized He-Ne laser (10 mW, 632.8 nm) beam is collimated and divided into the object and the reference beams. An optical microscope (Zeiss Axiostar) is inserted in the object arm of the Mach-Zehnder interferometer. The collimated object beam enters through the microscope illumination port. The reference

beam is reflected from a mirror that is attached to a piezo-transducer controlled with a computer for the phase-shifting. Samples are observed through a 40X, 0.65-NA microscope objective. The magnification factor can be changed easily by selecting a proper microscope objective as with conventional microscopes. The object and the reference beams are combined by a beam splitter placed in front of a CCD camera (Kodak MEGAPLUS 1.0/MV, 1008 × 1018 pixels, 9 μm × 9 μm pixel size, 8 bits). The full field of view of the system is 225 μm × 225 μm.

III. EXPERIMENTS

The in-line phase-shifting digital holographic microscopy system was used to measure the shape of a micro Fresnel lens formed on a polymethyl methacrylate (PMMA) base plate with an injection mold. The scanning electron microscope image of the injection mold is shown in Fig. 2. It has a center well and two grooves of 4.6 μm depth to produce a binary Fresnel lens. The radius of the center well is 23 μm and the inner and outer radii of the grooves are 32 and 40 μm and 46 and 51 μm. The refractive index of PMMA is 1.495. To measure the height profile of the micro Fresnel lens, distilled water was dropped onto the lens and a cover glass was placed on it as shown in the inset of Fig. 1.

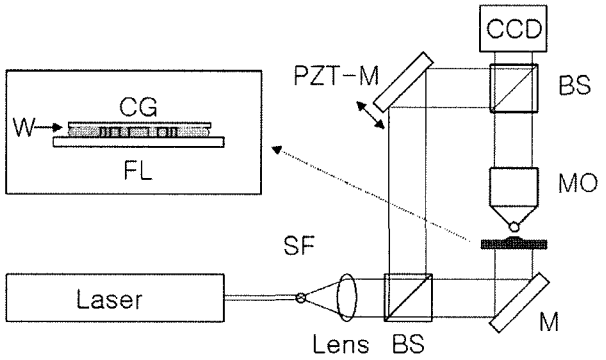

FIG. 1. In-line phase-shifting digital holographic microscope setup: SF, spatial filter; BS, beam splitter; M, mirror; PZT-M, PZT-attached mirror; and MO, microscope objective. Inset, prepared sample: CG, cover glass; W, water; and FL, micro Fresnel lens.

First, the complex object field on the CCD plane without the sample inserted was obtained from the four phase-shifted interference patterns whose intensity distributions are given by

$$I_n(x,y) = I_o(x,y) + I_r(x,y) + 2\sqrt{I_o(x,y)I_r(x,y)}\cos(\theta(x,y) + n\delta) \quad \text{with } n = 0,1,2,...3. \tag{1}$$

A sample interference pattern is shown in Fig. 3(a). In Eq. (1), $I_o(x, y)$, $I_r(x, y)$, and $\theta(x, y)$ are the object beam intensity, the reference beam intensity, and the initial phase difference between the object and the reference beams, respectively. δ is the step size of the phase-shift and about $\pi/2$. The phase-shifting errors can be corrected with a robust self-calibration algorithm [9]. The complex object field on the CCD plane, $U_0(x,y) = \sqrt{I_o(x,y)}\, e^{i\theta(x,y)}$, is obtained by using the same

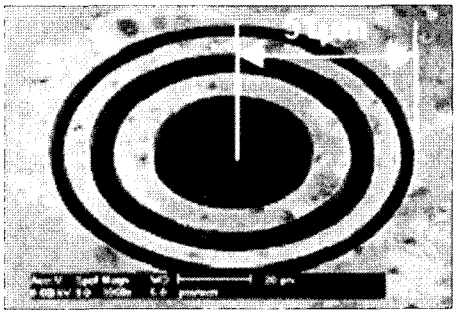

FIG. 2. SEM image of micro Fresnel lens insert mold.

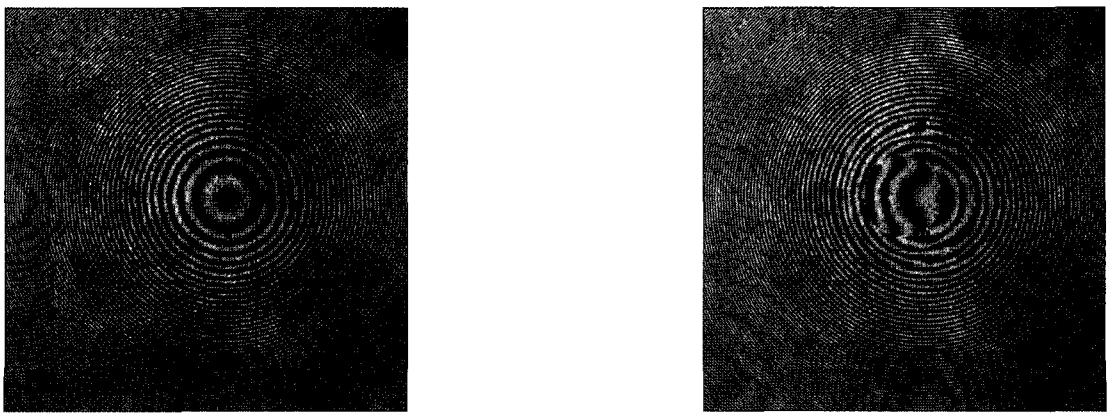

(a) (b)

FIG. 3. (a) Hologram without the lens. (b) Hologram including the lens.

algorithm.

Four more interference patterns are captured with the sample inserted. One of the four patterns is shown in Fig. 3(b). The complex amplitude on the CCD plane, $U_s(x,y) = \sqrt{I_o'(x,y)}\, e^{i[\varphi(x,y)+\theta(x,y)]}$ with the additional phase factor acquired from the lens $\varphi(x, y)$, is obtained similarly.

The object field on the plane containing the top of the Fresnel lens, $U_s(X, Y; Z)$, was numerically reconstructed from $U_s(x, y)$ using the plane wave expansion method devised in Ref. 10. We briefly describe the plane wave expansion method here. The object field on the hologram plane, $U(x,y) = u(x,y)e^{i\varphi(x,y)}$, is expressed as a Fourier integral:

$$U(x,y) = \int dk_x dk_y A(k_x,k_y) e^{i(k_x x + k_y y)}. \quad (2)$$

Its two-dimensional Fourier transformation, $A(k_x, k_y) = F_\perp\{U(x, y)\}$, is considered as the amplitude of the plane wave whose wave vector is $\vec{k} = k_x\hat{x} + k_y\hat{y} + k_z\hat{z}$ with $k_z = \sqrt{k^2 - (k_x^2 + k_y^2)}$ and $k = 2\pi/\lambda$. Then, the object field on the reconstruction plane is obtained as

$$U(X,Y;Z) = \int dk_x dk_y A(k_x,k_y) e^{i(k_x X + k_y Y)} e^{ik_z Z}. \quad (3)$$

In short, the object field on any reconstruction plane can be obtained from the following transformation of the object field on the hologram plane:

$$U(X,Y;Z) = F_\perp^{-1}\left\{F_\perp\{U(x,y)\} e^{ik_z Z}\right\}. \quad (4)$$

The merit of the plane wave expansion method is that there is no restriction on the propagation distance, Z.

IV. RESULTS

The value of Z(0.80 μm) that made the reconstructed sample image, $U_s(X, Y; Z)$, sharpest was used as the proper distance from the hologram plane to the sample plane. The object field on the same plane without the Fresnel lens inserted, $U_0(X, Y; Z)$, was reconstructed from $U_0(x, y)$ by the same method. Figure 4(a) shows the map of the wrapped phase difference between $U_s(X, Y; Z)$ and $U_0(X, Y; Z)$. Its unwrapped map, shown in Fig. 4(b), displays the distribution of the phase retardation acquired by the object field when it passes through the Fresnel lens. The horizontal and the vertical scales are in micrometers and the gray scales are in radians.

The thickness profile of the Fresnel lens was obtained from the relation between the phase difference $U_s(X, Y; Z)$ of and $U_0(X, Y; Z)$, α(X, Y), and the thickness of the lens, $l(X, Y)$:

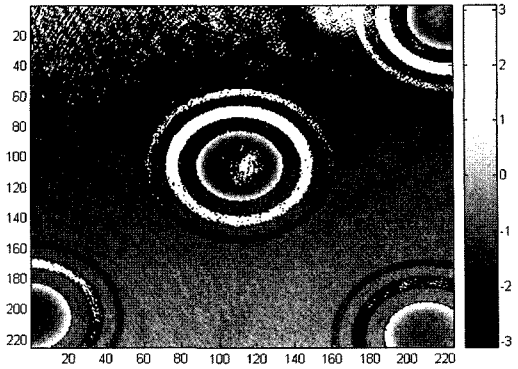

(a)

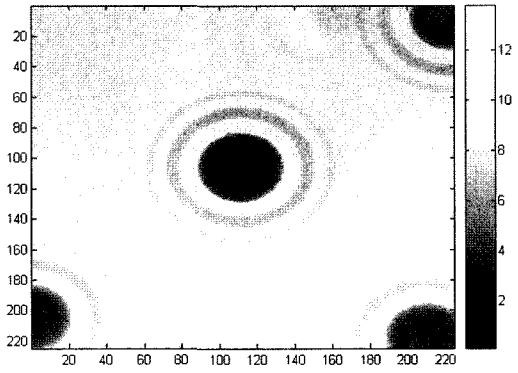

(b)

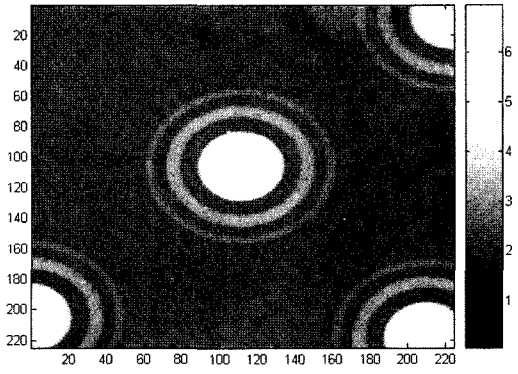

(c)

FIG. 4. (a) Subtracted phase after reconstruction. (b) Unwrapped phase of (a). (c) After removing the tilting error between the sample and cover glass, unwrapped phase of (b) is converted into thickness of lens.

$$\alpha(X,Y) = (n_l - n_w)kl(X,Y) + n_w kD(X,Y) + T(X,Y). \quad (5)$$

In Eq. (5), n_l (= 1.495) and n_w (= 1.333) are the refractive indices of the lens material, PMMA, and distilled water, respectively. $D(X, Y)$ is the total thickness of the sample including the Fresnel lens, distilled water, and the cover glass. The thickness of the cover

glass was not perfectly uniform and became a source of the lens thickness measurement error. Its standard deviation was measured to be 53 nm. $T(X, Y)$ represents the tilting between the lens base and the cover glass and can be removed by fitting a tilted plane to the flat region of the phase map. Through a calculation based on Eq. 5, the thickness distribution is shown in Fig. 4(c) after removing $T(X, Y)$. All scales are in micrometers.

The thickness profile of the micro Fresnel lens was obtained and shown in Fig. 5(a). The thickness profile along a line across the center is in Fig. 5(b) with the design profile of the insert mold. All numbers are in micrometers and the field of view is 112.5 μm × 112.5 μm. It can be seen that the thickness at the center of the lens is close to the design value of 4.6 μm. The shape of the lens is not the exact replica of the insert mold because its shape was deformed during the cooling down after the insert mold process. The Standard deviation of lens base thickness was 120 nm. Axial noise level is mainly determined by lens base and cover glass flatness (172 nm).

V. RESOLUTIONS

The lateral and the axial resolutions of our system were compared with those of an off-axis system. A USAF 1951 resolution target was measured through a 10x, 0.25-NA microscope objective lens having a theoretical resolution of 1.5 μm. The amplitude image in Fig. 6(a) was reconstructed from the four phase-shifted interference patterns. It can be seen that the smallest bars with about 2.2 μm spacing between them are clearly resolved. From the four phase-shifted interference patterns, one was selected as an off-axis hologram and the reconstructed amplitude image in Fig. 6(b) was obtained using the angular spectrum method of Ref. 8. It can be clearly seen that its overall image contrast is poorer than that of Fig. 6(a) and that the smallest bars are not clearly resolved especially in the horizontal direction according as the carrier fringes. In-line phase shifting method needs no filtering process and has the same resolution through horizontal and vertical directions.

The process was repeated without the sample in order to compare the noise levels of the systems. Figure 6(c) is the phase variation over a 180-μm length obtained with our process and Fig. 6(d) is that with the angular spectrum method. Reconstructed phase variation is 1.6° and 2.8° for each case. As expected, in-line phase shifting digital holography with a self-calibration algorithm gives higher axial resolution.

Phase-shifting digital holographic microscopy can examine the three-dimensional shape of a micro Fresnel lens with 1.6° phase resolution which corresponds to 17 nm height resolution in this measurement (PMMA-water) while maintaining the lateral resolution of con-

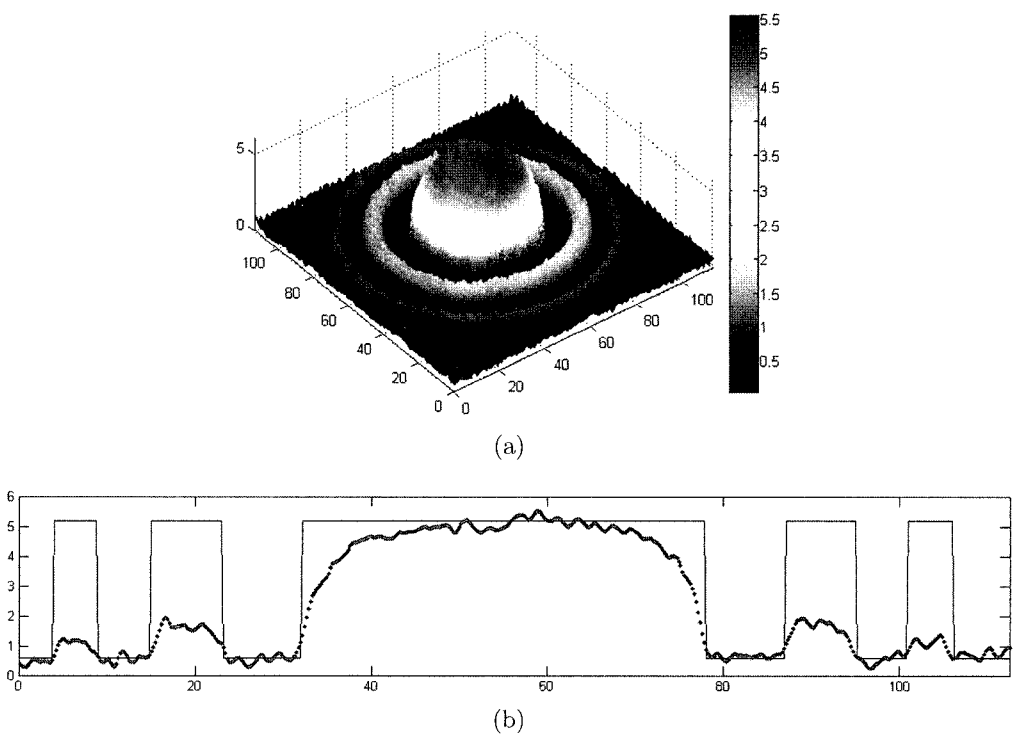

FIG. 5. (a) Three-dimensional shape of the lens. (b) Profile of the lens. Experimental values are compared with designed profile of the insert mold. All numbers are in micrometers.

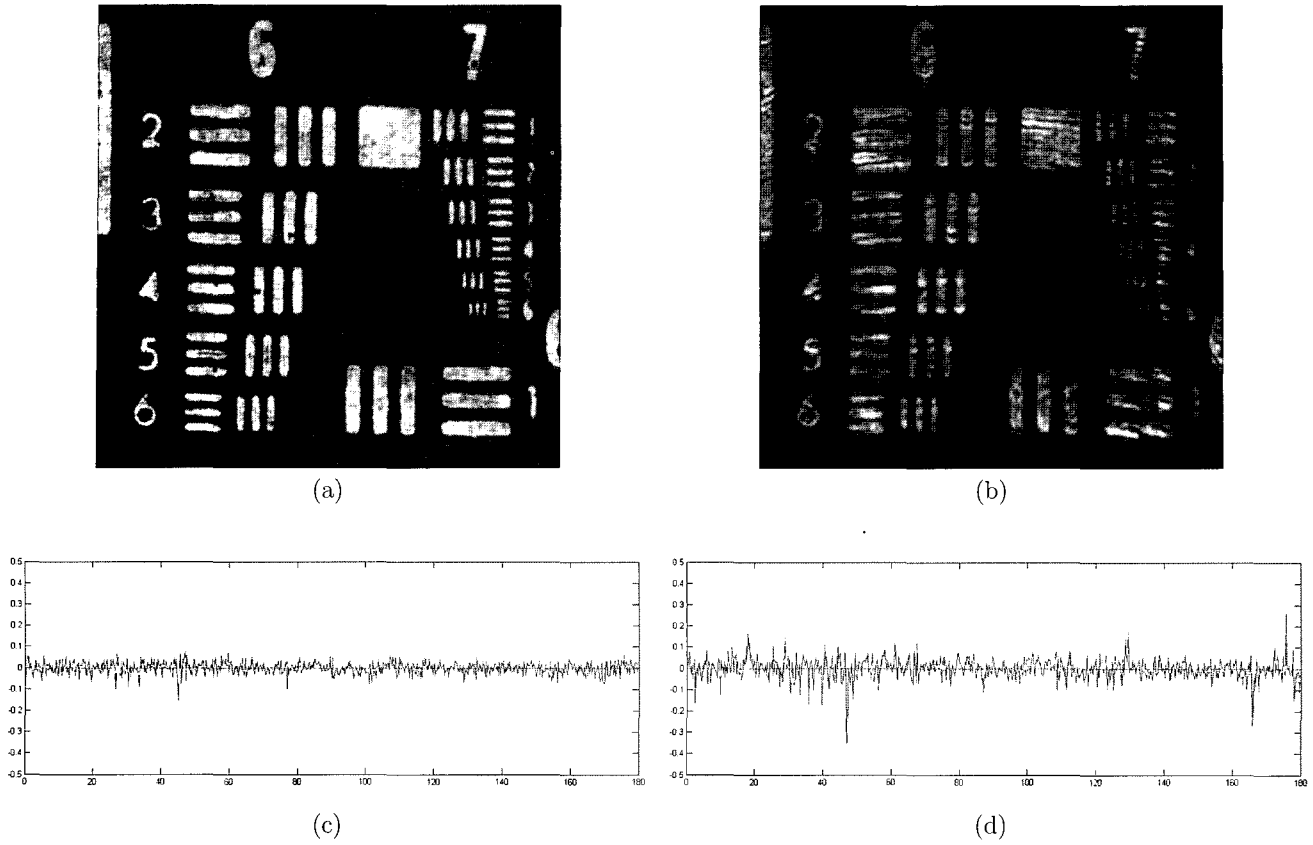

FIG. 6. (a) Reconstructed amplitude image of the resolution target with our method. All the bars are clearly resolved. (b) Reconstructed amplitude image of the resolution target with angular spectrum method. Overall contrast is much reduced and the smallest bars are not clearly resolved. (c) Reconstructed phase using in-line setup. (d) Reconstructed phase using off-axis setup.

ventional microscopy, 0.61 λ/NA (0.59 μm for 40x, 0.65 NA objective lens).

VI. CONLUSIONS

In summary, we have developed an in-line phase-shifting digital holographic microscopic system and measured the three-dimensional shape of a micro Fresnel lens. The use of an in-line configuration made it possible to estimate the complex object fields on the CCD plane with a phase-shifting method. A self-calibration algorithm was used to enhance the phase accuracy by eliminating the phase-shift error. The complex object fields on the sample plane reconstructed numerically from the complex object fields on the CCD plane had an axial resolution of 1.6°, higher than that could be obtained with off-axis digital holographic systems. This system can be applied to the precise three-dimensional shape measurement of any transparent microscopic object such as a micro-lens array, cells and to the observation of the dynamic change of microscopic objects.

ACKNOWLEDGEMENTS

We thank D. S. Kim, B. K. Lee and T. H. Kwon for supplying the micro Fresnel lens for the experiment. This work was supported by a grant No. 105025001 from Korea Science & Engineering Foundation.

*Corresponding author: ckho@postech.ac.kr

REFERENCES

[1] T. Wilson, ed., *Confocal Microscopy* (Academic Press, London,1990).

[2] P. K. Rastogi, ed., *Digital Speckle Pattern Interferometry and Related Techniques* (John Wiley & Sons, 2001).

[3] I. Yamaguchi and T. Zhang, "Phase-shifting digital holography," *Opt. Lett.*, vol. 22, no. 16, pp. 1268-1270, 1997.

[4] T. Zhang and I. Yamaguchi, "Three-dimensional microscopy with phase-shifting digital holography," *Opt. Lett.*, vol. 23, no. 15, pp. 1221-1223, 1998.

[5] I. Yamaguchi, J. Kato, S. Ohta, and J. Mizuno, "Image Formation in Phase-Shifting Digital Holography and

Applications to Microscopy," *Appl. Opt.*, vol. 40, no. 34, pp. 6177-6186, 2001.

[6] F. Charriere, J. Kuhn, T. Colomb, F. Montfort, E. Cuche, Y. Emery, K. Weible, P. Marquet, and C. Depeursinge, "Characterization of microlenses by digital holographic microscopy," *Appl. Opt.*, vol. 45, no. 5, pp. 829-835, 2006.

[7] P. Marquet, B. Rappaz, P. J. Magistretti, E. Cuche, Y. Emery, T. Colomb, and C. Depeursinge, "Digital holographic microscopy: a noninvasive contrast imaging technique allowing quantitative visualization of living cells with subwavelength axial accuracy," *Opt. Lett.*, vol. 30, no. 5, pp. 468-470, 2005.

[8] C. Mann, L. Yu, C. Lo, and M. K. Kim, "High-resolution quantitative phase-contrast microscopy by digital holography," *Opt. Express*, vol. 13, no. 22, pp. 8693-8698, 2005.

[9] H. Y. Yun and C. K. Hong, "Interframe intensity correlation matrix for self-calibration in phase-shifting interferometry," *Appl. Opt.*, vol. 44, no. 23, pp. 4860-4869, 2005.

[10] H. Y. Yun, S. J. Jeong, J. W. Kang, and C. K. Hong, "3-dimensional micro-structure inspection by phase-shifting digital holography," *Key. Eng. Mater.*, vol. 270-273, pp. 756-761, 2004.